Modelling the impact of historical and future Land Use Land Cover changes on the hydrological response of an Ethiopian watershed

Motuma Shiferaw Regasa[1], Michael Nones [2,*]

[1] Department of Hydrology and Hydrodynamics, Institute of Geophysics, Polish Academy of Science, Warsaw, Poland; Ksiecia Janusza 64, 01-452 Warsaw, Poland; e-mail: mregasa@igf.edu.pl; ORCID 0000-0002-6955-6838

[2] Department of Hydrology and Hydrodynamics, Institute of Geophysics, Polish Academy of Science, Warsaw, Poland; Ksiecia Janusza 64, 01-452 Warsaw, Poland; phone: +48226915776; e-mail: mnones@igf.edu.pl; ORCID 0000-0003-4395-2637 (author for correspondence)

Abstract

Land Use Land Cover (LULC) is generally considered one of the key factors influencing the hydrological processes and sediment output in arid and semi-arid watersheds. Focusing on the Ethiopian Fincha watershed, the current study applies the Soil & Water Assessment Tool (SWAT) model to evaluate how LULC changes affect the watershed hydrological dynamics. Utilizing the available stream flow time series data acquired from 1986 to 2008, the model was calibrated and validated based on past conditions. At the same time, future scenarios were simulated by means of the Land Change Modeler (LCM) model using historical trends. To investigate the effect of LULC changes on watershed hydrology, six LULC maps have been produced to account for historical (1989, 2004, 2019) and future (2030, 2040, 2050) conditions. The results show an increase in surface runoff in the past, while a similar tendency is expected for the next three decades if no

specific mitigation measures will be implemented soon. On the other hand, lateral flow and groundwater flow are generally decreasing. The present analysis shows that the ongoing LULC transformation, which involves an expansion of agricultural land, urban areas, and intermittent logging of forest cover, may be the reason for the increment in surface runoff, and the decline in groundwater and lateral flow.

Keywords

Ethiopia; Fincha watershed; hydrology; Land Use Land Cover; Sediment yield; Soil and Water Assessment Tool

1. Introduction

One of the most important components of the terrestrial ecosystem, Land Use and Land Cover (LULC), has a significant impact on a variety of processes, including the hydrological cycle, geomorphological processes, land productivity, and animal species (e.g., Garg et al., 2019; Kenea et al., 2021; Leta et al., 2021; Regasa et al., 2021; Katna et al., 2023). There have been noticeable changes in land cover throughout the world because of the high demand placed on land resources to provide food, water, and shelter for the growing world population (Dibaba et al., 2020; Regasa & Nones, 2022). These changes affect the sediment production levels, as well as the hydrological regimes of the watersheds. The increasing use of land as an agricultural resource to face the population growth at the expense of a more natural plant coverage is significantly increasing the surface erosion across Ethiopian watersheds (e.g., Etter et al., 2006; Schielein & Börner, 2008; Rodrguez et al., 2013; Kouassi et al., 2021; Abdurahman et al., 2023). In addition to LULC, human-caused climate change is one of the most important factors influencing changes in runoff, according to Dibaba et al. (2020). The peculiarities of the local watershed and the agro-ecological settings should also be considered in evaluating how much LULC and/or climate change affect changes in basin-wide runoff (Berihun et al., 2019; Aragaw et al., 2021; Shitu & Berhanu, 2023). Moreover, it is worth reminding the excessive pressure from abstraction, drainage, dredging, contamination, silting, and introduction of alien species is also a major issue in river basin management, as it has already caused the collapse of freshwater ecosystems worldwide (Agashua et al., 2022).

According to Regasa et al. (2021), Ethiopia is severely affected by LULC changes, eventually resulting in significant landscape transformation, and harming its key water resources, including the Blue Nile Basin, a major natural resource of the country. Variations in interception, infiltration, evapotranspiration, and groundwater recharge that are linked to LULC changes are the primary causes of catchment-wise hydrological changes, claims a study performed by Leta et al. (2022). Therefore, assessing how LULC changes affect hydrology is crucial for understanding the current implications of landscape transformation on water resources, as well as creating effective watershed management strategies and conservation initiatives. However, such an assessment might be complicated by the lack of measured data, a common feature in developing countries like Ethiopia (Eshete et al., 2022).

With the use of hydrologic models, it is possible to spatially map the patterns of hydrological implications brought on by LULC changes as well as compare changes in basin-scale LULC with response in hydrological components. Previous studies used a variety of hydrologic models, including the Soil and Water Assessment Tool (SWAT) (Baker & Miller, 2013; Cuceloglu et al., 2017; Shi et al., 2017; Khoury et al., 2023), the Système Hydrologique Européen (MIKE-SHE) (Zhang et al., 2021) and the Distributed Hydrology-Soil-Vegetation Model (DHSVM). In their work, Aawar & Khare (2020) used SWAT to analyze the effects of LULC changes on the hydrology of the Kabul River, a 700-kilometre-long tributary to the Indus River in Pakistan. Their results demonstrated how climate change affects water resources significantly because it not only affects precipitation and temperature but also directly affects stream flow. The SWAT hydrologic model was used to evaluate and spatially map the effects of changes in farmlands and urban areas on stream flow in the Ethiopian River basins (e.g., Abuhay et al., 2023; Tola & Shetty, 2023; Gurara et al., 2023). In previous investigations MODFLOW and SWAT were loosely coupled to estimate recharge and ascertain the impact of groundwater abstraction and recharge on groundwater levels (Nyakund et al., 2022).

Despite the extensive literature on 0the Blue Nile Basin's water resources, the majority of these studies have not focused on how specific LULC classes influence the basin's hydrological components. In fact, past investigations (e.g., Dibaba et al., 2020; Maru et al., 2023) were more focused on considering only past and present LULC conditions in evaluating basin-wide hydrological response, without providing possible future scenarios. However, to create sustainable water resource and land-use planning strategies and safeguard the area from the detrimental effects of anthropogenic activities on ecosystem functions, information on the future effects of LULC on the hydrology of the Fincha watershed is needed. Therefore, this study combines past LULC maps with future scenarios to model the hydrological response of the data-scarce Fincha watershed. The SWAT model was here applied because of its i) free availability; ii) simple GIS-based interface integration; and iii) connection tools for sensitivity, uncertainty, validation, and calibration. Moreover, as past studies demonstrated (Eshete et al., 2022), SWAT implementation is relatively simple also in data-poor regions, such as the Fincha watershed.

2. Materials and Methods

2.1 Study Area

The Fincha watershed is situated in Ethiopia's Oromia Regional State's Horro Guduru Walaga Zone, which is part of the Upper Blue Nile Basin. It lies roughly 300 kilometres from Addis Ababa, the country capital, between latitudes 9°9′53″ N and 10°1′00″ N and longitudes 37°00′25″ E and 37°33′17″ E (Figure 1).

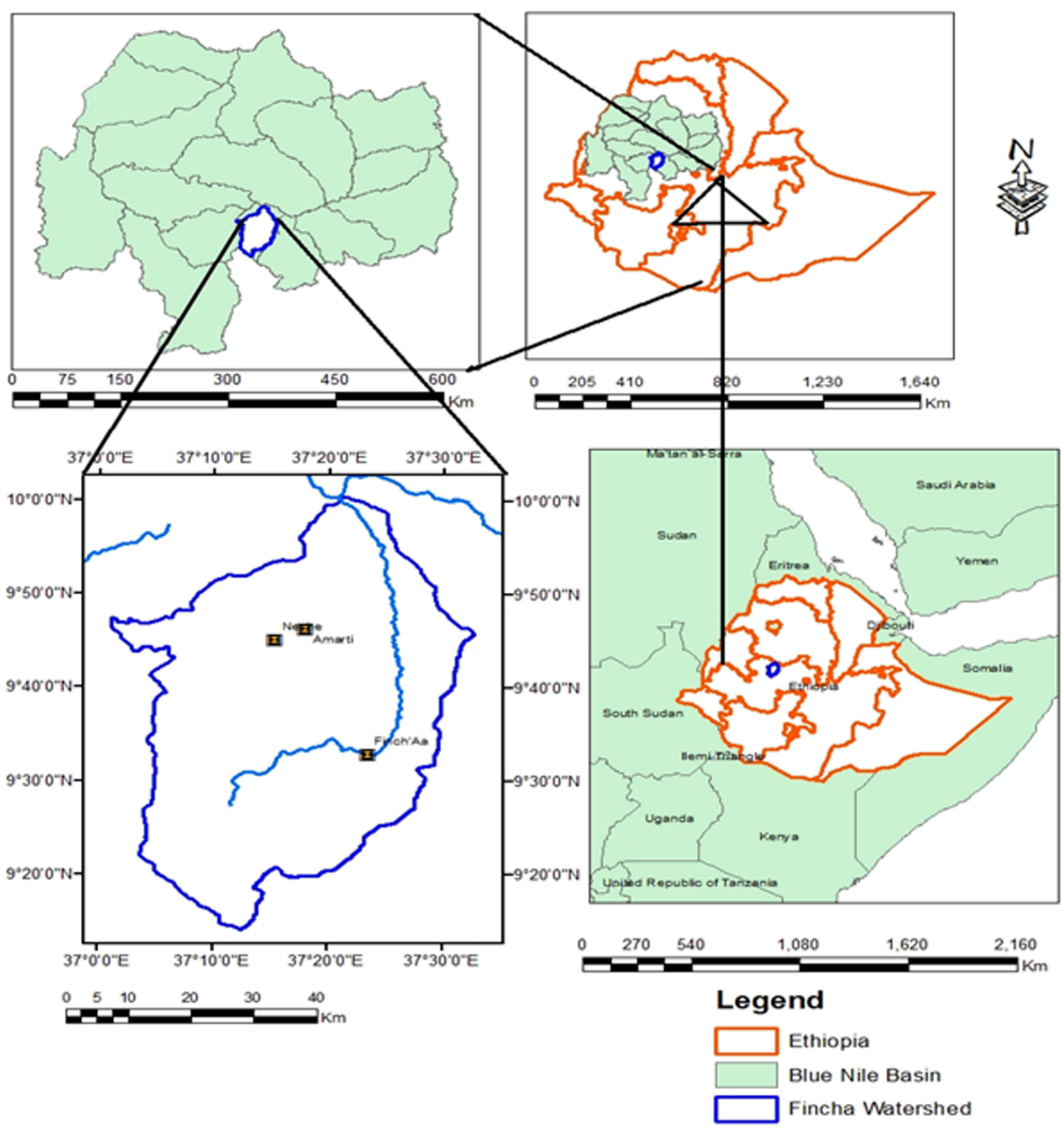

Figure 1. Location of the Fincha watershed, Oromia Regional State's Horro Guduru Walaga Zone, Upper Blue Nile Basin, Ethiopia.

The region is characterized by four distinct seasons: Summer, from June to August, with heavy rains; Autumn, from September to November, is the harvest season; Winter, from December to February, the dry season characterized by morning frost; Spring, from March to May, very hot and with scattered rains. The annual rainfall ranges from 1367 to 1842 mm, with the Northern lowlands receiving the least rain and the Southern and Western highlands receiving more than 1500 mm per year (Regasa & Nones, 2022). The major rainy season lasts from June through September, with an average of 1604 mm of precipitation, with a maximum in July and August.

Due to its downstream connection to the Nile River Basin and the extensive agriculture in the area, the Fincha watershed has national and international significance in hydro-politics. Large-scale sugar cane fields are irrigated using natural resources such as the Fincha, Amerti, and Nashe lakes (Leta et al., 2021; Regasa & Nones, 2022). These lakes also contribute to the national economy by producing hydroelectric power.

2.2 Available dataset

The SWAT model requires multiple inputs, summarized in Table 1. In detail, a 30m-resolute Digital Elevation Model (DEM), LULC maps, soil data, weather data (relative humidity, precipitation, solar radiation, temperature, wind speed) and stream flow data. Apart from LULC maps, the remaining data were collected from the Ethiopian Ministry of Water, Irrigation and Energy Department (MOWE). LULC maps were prepared by classifying Landsat images freely obtained from the United States Geological Survey website (earthexplorer.usgs.gov).

The study workflow is summarized in Figure 2, where green boxes represent input data, red boxes are the used models, and blue boxes summarize the outcomes.

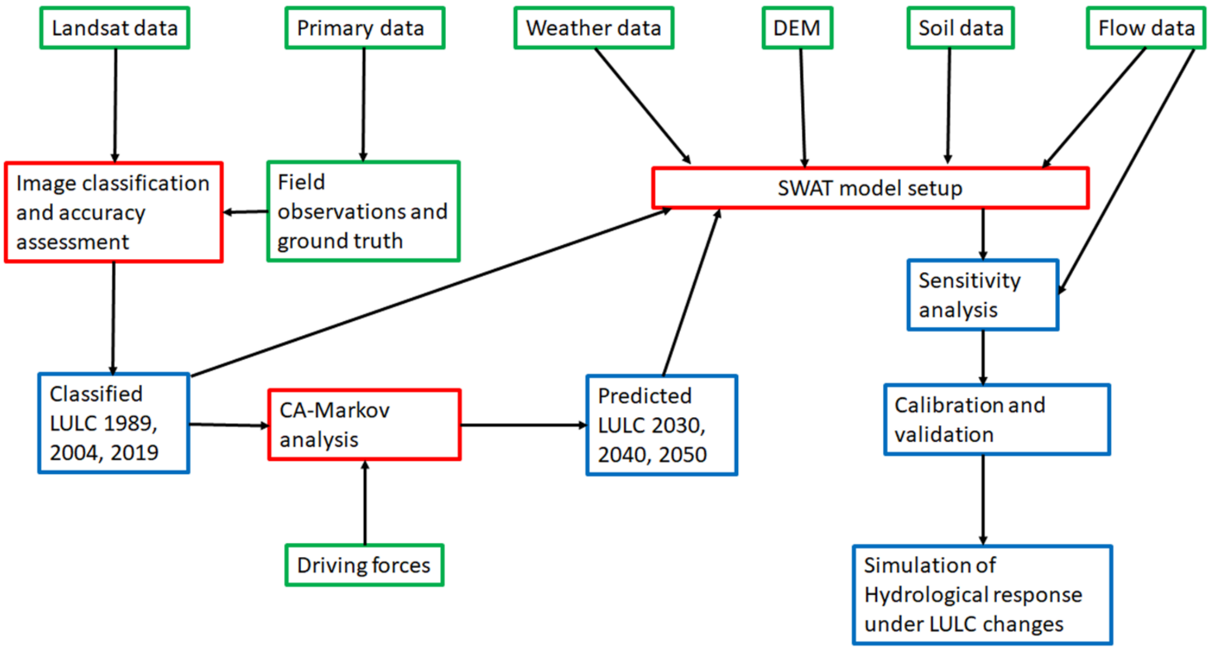

Figure 2. Study workflow.

Table 1. Data and sources.

Data	*Type*	Resolution/year	*Source*
Digital Elevation Model	Spatial Data	30m / 2019	Ministry of Water and Energy (MOWE), Ethiopia
Land use land cover	Spatial Data	30m / 2019, 2030, 2040, 2050	2019 derived from Landsat images 2030, 2040, and 2050 predicted by Land Change Modeler (Regasa and Nones, 2022)
Soil	Spatial Data		Ministry of Water and Energy (MOWE), Ethiopia
Weather data	Temporal data	1986-2019	Meteorological National Agency, Ethiopia
Stream flow	Temporal data	1986-2008	Ministry of Water and Energy (MOWE), Ethiopia

2.2.1 Weather data

The study was performed using daily weather observations measured from 1986 to 2019 in ten gauging stations (namely, Fincha, Alibo, Gebete, Homi, Hareto, Jermet, Nashe, Kombolcha, Shambu, and Wayyu). In detail, the hydrological balance was calculated using daily rainfall, minimum and maximum temperatures, wind speed, relative humidity, and sun radiation. Xlstat, a statistical program, was employed to fill gaps where measured data was absent.

2.2.2 Soil data

According to Pennock (2019), soil data were pre-processed using the Food and Agricultural Organization (FAO) standards. Ten different soil types are found in the Fincha watershed: Eutric Cambislos, Dystric Vertisols, Eutric Vertisols, Eutric Leptosols, Haplic Arenosols, Haplic Phaeozems, Chromic Luvisols, Water, Rhodic Nitisols, and Marsh (Figure 3). However, Haplic Alisols and Eutric Cambislos make up most of the watershed.

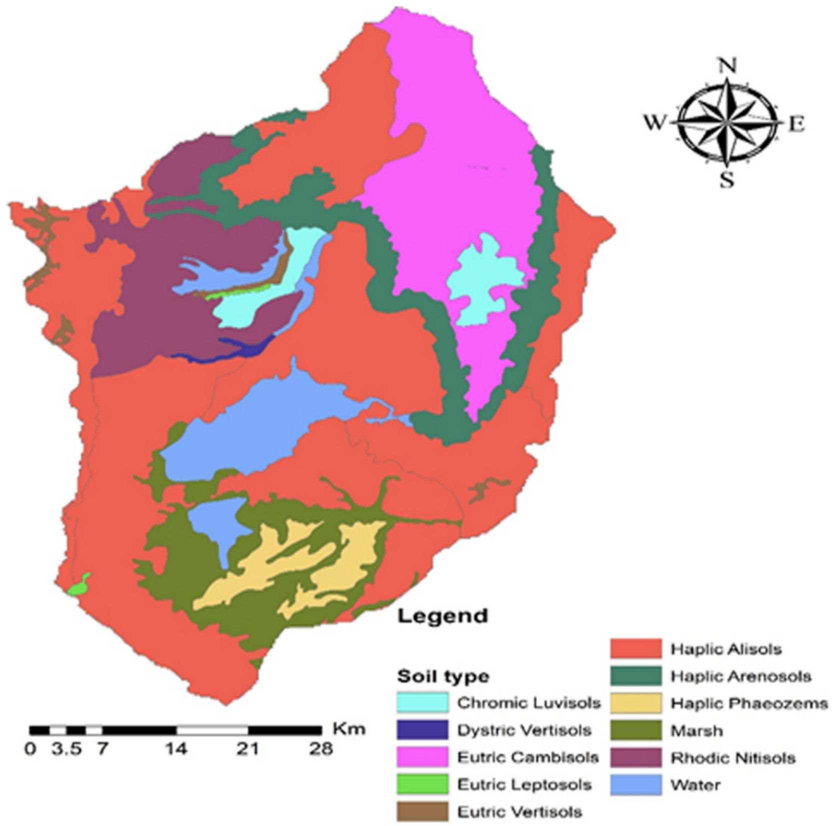

Figure 3. Soil types characterizing the Fincha watershed.

2.2.3 Land Use Land Cover

Land use affects surface runoff, evapotranspiration, erosion, nutrients, and pesticide burden in a watershed. Landsat images (Landsat 5 for 1989 and 2004, Landsat 8 for 2019) were freely downloaded from the official web page of the United States Geological Survey (USGS) (earthexplorer.usgs.gov) and then handled using Arc-GIS. Based on these images, the LULC maps of 1989, 2004 and 2019 were created, accounting for six classes: water body, grass/swamp, built-up, agricultural land, woodland, and shrub. Given that SWAT requires standard designations (WATR, WETL, URBN, AGRL, FRSE, FRST) the maps were reclassified, considering water body, grass/swamp, built-up, agricultural land, forest and shrub, respectively (Figure 4).

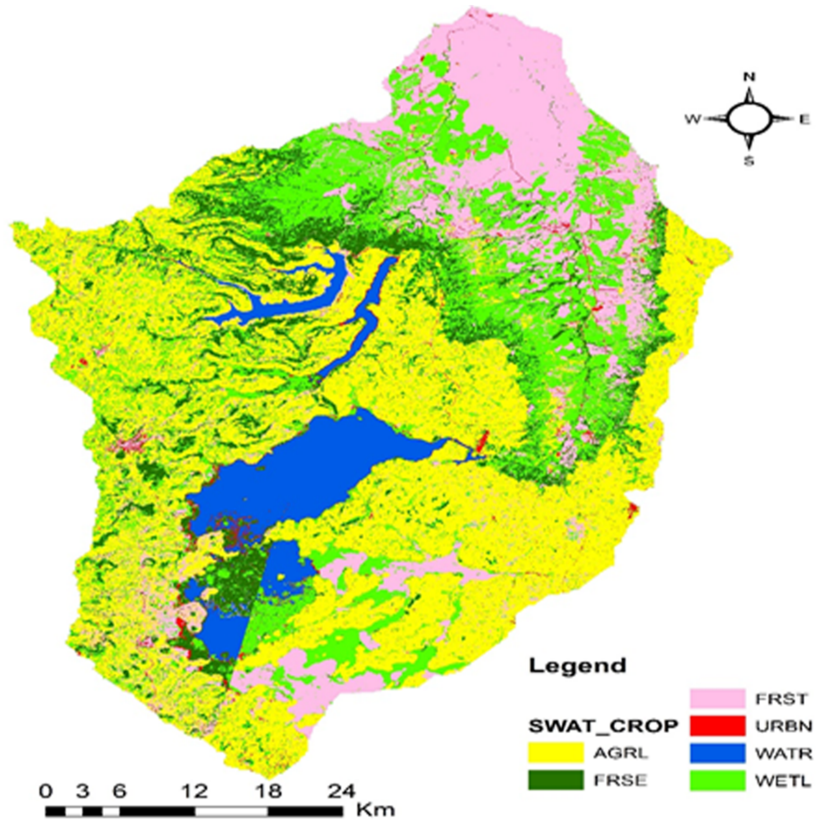

Figure 4. 2019 LULC map of the Fincha watershed.

Earlier studies (Desalegn et al., 2014), information obtained from Key Informant Interviews with seniors who have known the area for at least three decades and from Focal Group Discussions with various office and local representatives, as well as ground truth data obtained during field campaigns performed in 2020 and 2021, were used to support the present classification.

As described in detail in Regasa & Nones (2022), future LULC maps were predicted via the Land Change Modeler using the historical maps and accounting for different driving variables (distance from the disturbance, distance from stream, distance from urban, distance from road, Evidence likelihood, elevation and slope). The LCM was applied to predict LULC scenarios for 2030, 2040 and 2050 following a few key steps: i) analysis of past LULC maps (1989, 2004, 2019) and related changes; ii) creation of change probability matrixes, iii) evaluation of model performances; iv) predication of future LULC maps considering multiple potential drivers.

2.2.4 Slope

Using a 30m x 30m DEM of the Fincha watershed and the Arc-GIS spatial analysis tool, four slope categories were selected (<10%, 15%, 25%, >30%) based on previous works (Kenea et al., 2021), as these categories are considered representative of the Fincha watershed's topography (Figure 5).

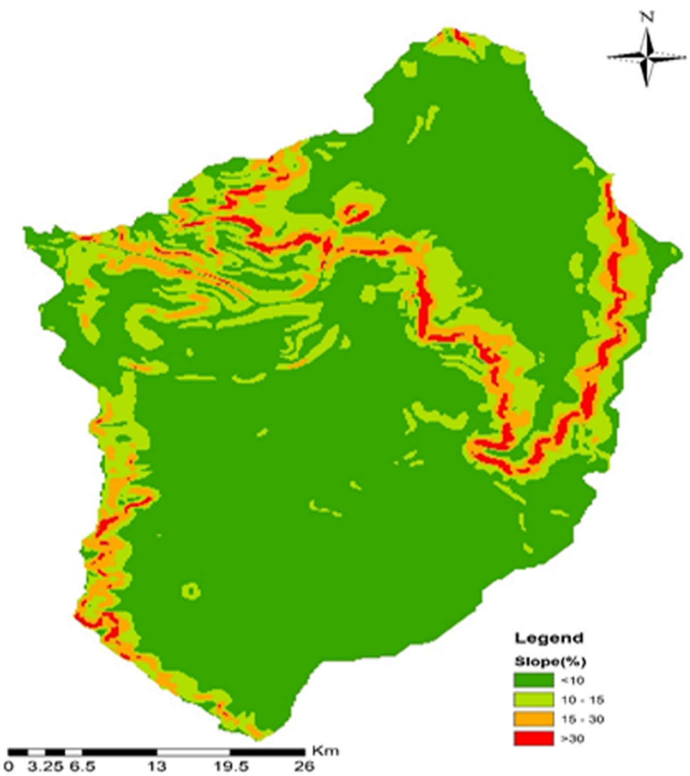

Figure 5. Classification of the Fincha watershed based on terrain slope.

2.3 SWAT model setup

The United States Department of Agriculture (USDA) developed the Soil and Water Assessment Tool (SWAT), a continuous-time, semi-distributed, process-based watershed model, to predict the sediment, impact of land management practices on water, and chemical vintages in agricultural watersheds (Neitsch et al., 2011; Tadesse et al., 2015). SWAT is usually used to recognize the hydrological cycle, simulating the effect of land use, water quality, and ecosystem drivers on the hydrology, to eventually derive sediment yield and soil management practices (e.g., Woldesenbet et al., 2017; Dibaba et al., 2021; Tola & Shetty, 2023).

Within a watershed, SWAT considers sub-watersheds that are connected by a stream channel. Subsequently, each sub-watershed is further divided into Hydrologic Response Units (HRU), depending on the local specific configuration of soil, land use and slope type (Tibebe & Bewket, 2011; Megersa et al., 2019). Groundwater, water yield, lateral flow, evapotranspiration, surface runoff, and sediment are all simulated by SWAT at the HRU level. The outputs are averaged at the sub- and watershed levels before being directed via the stream network. SWAT use the following equation of water balance to simulate the hydrological cycle:

$$SW_t = SW_o + \sum_{i=1}^{t}(R_{day} - Q_{surf} - E_a - W_{seep} - Q_{gw}) \quad (1)$$

where SW_t indicates the most recent soil water content (mm), SW_o is the soil water content of the first day of simulation (mm), t represents the number of days, R_{day} is the daily precipitation (mm), Q_{surf} indicates the daily surface runoff (mm), W_{seep} is the daily value of water entering the vadose zone from the soil profile (mm), E_a represents the daily evapotranspiration (mm), and Q_{gw} is the daily groundwater flow (mm).

2.3.1 Watershed delineation

The stream network was built in SWAT using the 30m-resolution DEM of the Fincha basin (Table 1), and the watershed and sub-watersheds were defined considering flow accumulation and water flow direction. Watershed and sub-watershed boundaries were established using several procedures, such as DEM setup, stream definition, drainage pattern, inlet and outlet definition, watershed outlet selection and definition (Figure 6).

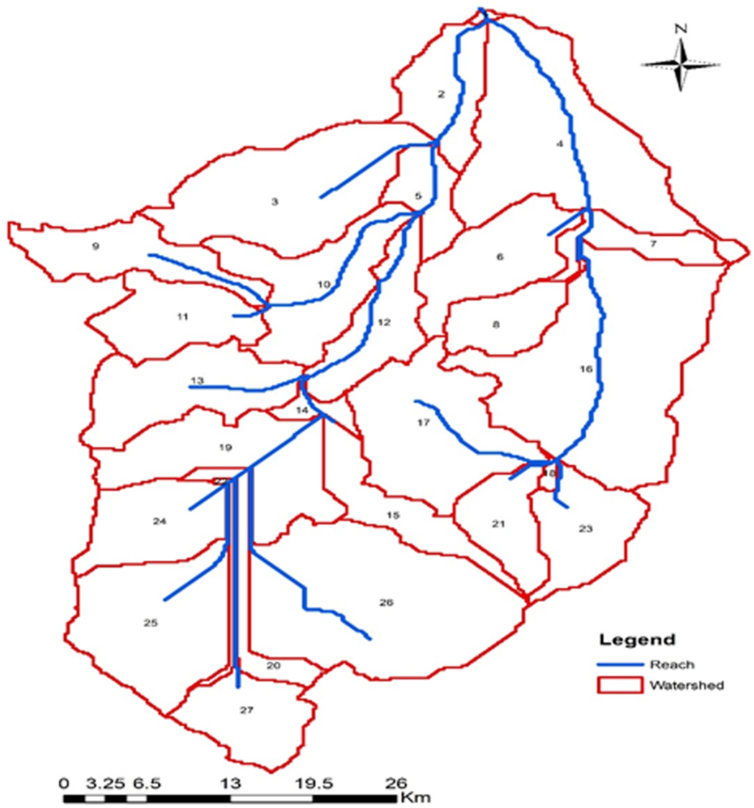

Figure 6. River drainage system (blue lines) and sub-watersheds (red contours).

2.3.2 Hydrologic Response Units

Using the DEM, the LULC maps and the soil map, different HRUs were calculated, as they depend on soil, land use and slope type. According to Leta et al. (2021), areas with low land uses and slope classes can be eliminated when establishing HRUs by applying a 10% criterion. The Fincha watershed was consequently split into 234 HRUs, which were then merged into 27 sub-watersheds.

2.3.3 Sensitivity analysis

Determining the model's most significant parameters is known as a sensitivity analysis (Hamby, 1994). As made in similar studies (Dibaba et al., 2020; Leta et al., 2021; Barman et al., 2023), this sensitivity analysis was performed using the SUFI-2 (Sequential Uncertainty Fitting-2) technique, an interface of SWAT-CUP (SWAT-Calibration Uncertainty Program), and evaluating the utmost significant hydrological parameters. *T*-statistics and *p*-value statistics, respectively, provided the measure and significance of sensitivity, according to earlier studies (e.g., Khalid et al., 2016; Gyamfi et al., 2016; Khalilian & Shahvari, 2018; Sharma et al., 2023). Following previous investigations (Regasa & Nones, 2023), nine parameters were selected (Table 2).

Table 2. Stream flow characteristics with range and fitted value, as determined by the SUFI-2-based sensitivity study. The absolute value of the *p*-value was used to determine their ranking.

Rank	Parameter Name	Description	Calibration	
			t-stat	*p*-value
1	V_GW_DELAY.gw	Groundwater delay (days)	-9.891	0.000
2	R_CN2.mgt	SCS runoff curve number II	2.391	0.018
3	V_GWQMN.gw	Threshold depth of water in the shallow aquifer required for return flow to occur (mm H2O)	-2.022	0.045
4	R_CH_N2.rte	Manning's "n" value for the main channel	0.717	0.474
5	R_SOL_AWC(1).sol	Available water capacity of the 1st soil layer (mm H2O mm soil−1)	0.699	0.486
6	R_SOL_K(1).sol	Saturated hydraulic conductivity at the 1st soil layer (mm h−1)	0.255	0.799
7	R_SLSUBBSN.hru	Average slope length (m)	0.153	0.878
8	R_RCHRG_DP.gw	Deep aquifer percolation fraction	-0.099	0.921
9	V_ALPHA_BF.gw	Base flow alpha factor(1 day−1)	0.060	0.952

2.3.4 SWAT Calibration and validation

The stream flow data were acquired from MOWE, and refer to the period 1986-2008, while more recent data are not available. These data were divided into two periods, considering an additional initial warm-up phase. Specifically, the first three years (1986-1988) served as the initiation period, 1989-2002 as the calibration period, and 2003-2008 as the validation period. To estimate the standard of fit between monthly simulated and observed data, the model efficiency was judged using the determination of coefficient (R^2, eq. 2), the Nash-Sutcliffe simulation efficiency (*NSE*, eq. 3), and the per cent bias (*PBIAS*, eq. 4).

The determination coefficient (eq. 2) can range from 0 (inadequate model) to 1 (perfect fit between model and real data), and, typically, $R^2>0.6$ means a good correlation (Leta et al., 2021, Regasa & Nones, 2022).

NSE (eq. 3) values can reach a maximum of 1, with positive *NSE* meaning that the model executes better than the ideal fit derived from the data average used as a predictor, and negative values indicating that the model performs worse than the ideal fit (Jilo et al., 2019). Four levels of simulation efficiency can be considered: unsatisfactory ($NSE<0.50$), satisfactory ($0.5<NSE<0.65$), good ($0.65<NSE<0.75$), and very good ($0.75<NSE<1$), as suggested by past studies (Leta et al., 2021; Regasa & Nones, 2022).

PBIAS (eq. 4) measures the typical likelihood of the simulated data deviating from the observed data in size or frequency, while lower *PBIAS* denotes better simulation outcomes.

$$R^2 = \left[\frac{\sum_{i=1}^{n}(Q_{Obs} - \bar{Q}_{Obs})(Q_{cal} - \bar{Q}_{Cal}}{\sum_{i=1}^{n}(Q_{Obs} - \bar{Q}_{Obs})^2 \sum_{i=1}^{n}(Q_{Cal} - \bar{Q}_{Cal})^2}\right]^2 \quad (2)$$

$$A = 1 - \frac{\sum_{i=1}^{n}(Q_{Obs} - Q_{Cal})^2}{\sum_{i=1}^{n}(Q_{Obs} - \bar{Q}_{Obs})^2} \quad (3)$$

$$PBIAS = \frac{\sum_{i=1}^{n}(Q_{Obs} - Q_{Calc}) * 100}{\sum_{i=1}^{n} Q_{Obs}} \quad (4)$$

where Q_{Obs} represents the actual variable, $\overline{Q}_{Obs}$ represents its time average, Q_{Cal} represents the simulated variable and $\overline{Q}_{Cal}$ represents its time average.

2.4 Scenarios simulation

It is critical to consider how LULC change affects hydrological processes in basins and watersheds for the proper management of water resources (Garg et al., 2019). The calibrated and verified model, along with LULC maps for 1989, 2004, 2019, 2030, 2040, and 2050, was employed to evaluate how LULC alterations affected the hydrology of the watershed. The consequences change of LULC were evaluated at the watershed level using the simulated findings, and the effect of individual modifications at the sub-watershed scale was identified.

Mimicking similar approaches (Leta et al., 2021), the goal of the present research was to explore the effects of LULC modification using a fixing-changing methodology. Therefore, only the LULC maps were altered here, while all other input model parameters were left unchanged.

Through scenario-based simulations, the effects of trend and predicted LULC shifts on watershed/sub-watershed hydrological responses for the past (1989 to 2019) and future (2030 to 2050) conditions were assessed. ArcGIS was used to categorize the LULC of the Fincha watershed and Land Change Modeler (LCM) to predict it for the coming years (2030, 2040, 2050) using data from previous Landsat images (1989, 2004, 2019).

Five Scenarios (two for the past and three for the future) were developed to analyze the hydrological response of the Fincha watershed under LULC changes: past scenarios refer to the periods 1989-2004 and 2004-2019, while future scenarios consider the periods 2019-2030, 2030-2040 and 2040-2050.

3. Results

3.1 Historical and future trends of LULC

Comparing the six reference years, it is possible to observe significant changes in LULC, with an increment in areas covered by settlements, agricultural fields, water bodies and grass. At the same time, a decrement in natural coverage (forest and shrubs) is observable (Figure 7).

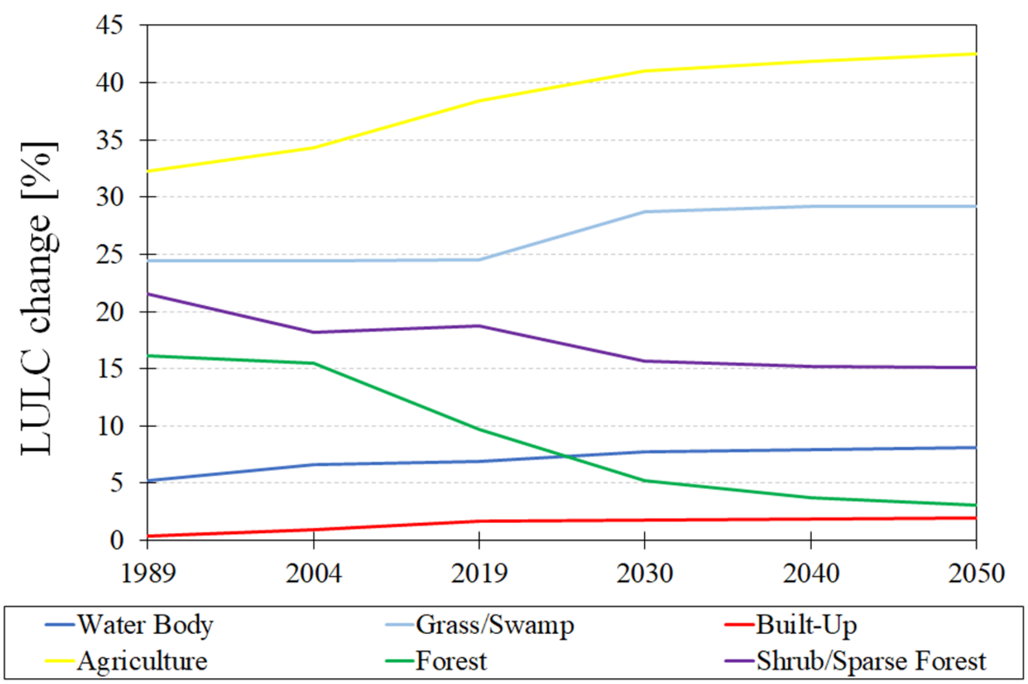

Figure 7. Historical (1989-2019) and predicted (2030-2050) LULC changes in the Fincha watershed.

A more in-depth analysis of such trends is reported in Regasa & Nones (2022), and their results are used here for inferring the hydrological response of the basin to such LULC changes.

3.2 SWAT Calibration and validation

Using the measured monthly stream flow at the Fincha reservoir close to the Fincha Dam outlet (Figure 1) from 1986 to 2008. The warm-up period, from 1986 to 1988, was used to lessen the impact of the beginning conditions during the model's initial stage. Following this, the calibration and validation periods ran from 1989 to 2002 and 2003 to 2008, respectively.

Looking at Table 3, one can notice that the R^2 values obtained for both calibration and validation, show good correlation. This is confirmed also by the high values of *NSE* and the reduced *PBIAS*.

Table 3. Monthly stream flow during the calibration (1989-2002) and validation (2003-2008) periods.

	Statistical test	R^2	*NSE*	*PBIAS*
Stream flow	Calibration	0.83	0.83	8.3
	Validation	0.84	0.76	12.2

Figure 8 reports the computed and measured monthly stream flow at the Fincha Dam outlet, showing that SWAT is generally able to reproduce the observed behaviour, even if some peaks are not well represented, especially during the calibration phase.

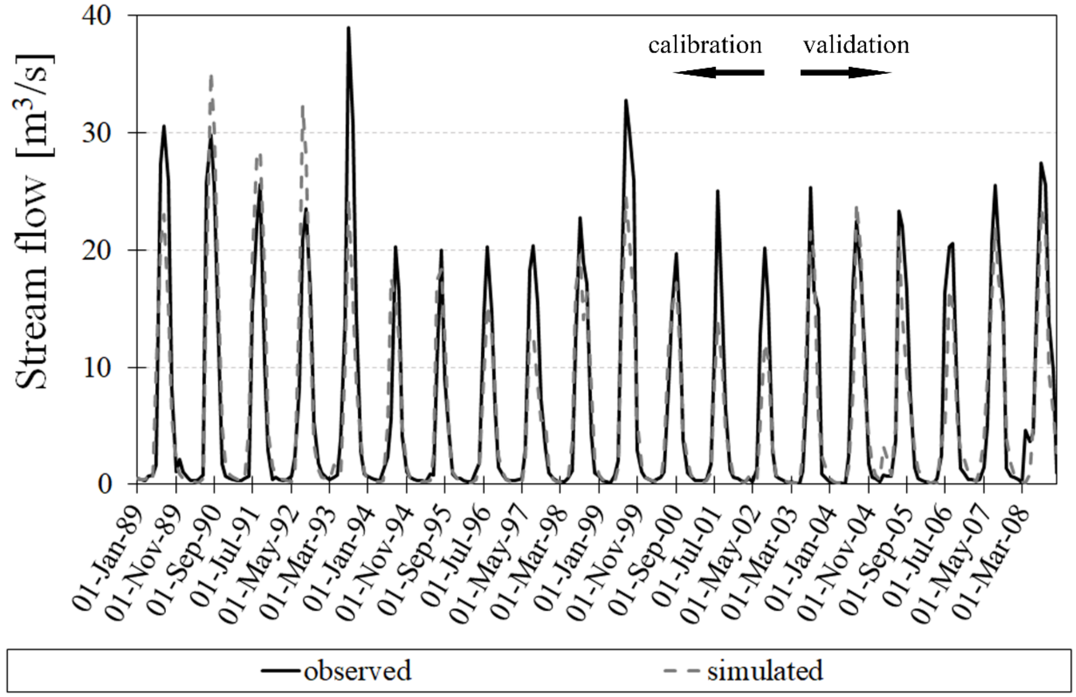

Figure 8. Comparison between computed and measured stream flow at the Fincha Dam outlet, during the calibration (1989-2002) and validation (2003-2008) periods.

3.3 Effects of Land Use Changes on Hydrological Components

Following similar investigations (Leta et al., 2021; Kuma et al., 2023), it was assumed here that hydrological component fluctuations were only due to LULC changes, to be able to uncouple the effects of LULC and climatic change. Therefore, the scenarios simulations were run with constant meteorological data, changing only LULC conditions.

Because of more significant LULC alterations, the simulated surface runoff for future LULC scenarios was higher than the one modelled for past conditions. Specifically, in comparison to the previous scenarios, future scenarios (2030, 2040, 2050) produce more surface runoff and less groundwater flow (Table 4).

Table 4: Fincha watershed's average annual hydrological components.

Hydrological components	Hydrological components [mm]						Hydrological components change [%]				
	1989	2004	2019	2030	2040	2050	2004-1989	2019-2004	2030-2019	2040-2030	2050-2040
Surface runoff	370.13	385.25	405.15	424.99	433.09	435.14	4.08	5.17	4.90	1.90	0.47
Lateral flow	42.52	40.26	40.04	36.14	33.38	32.73	-5.32	-0.55	-9.73	-7.64	-1.94
Groundwater	480.73	469.09	450.51	433.89	426.76	423.43	-2.42	-3.96	-3.69	-1.65	-0.78
Water yield	920.35	920.95	921.07	919.53	917.34	916.25	0.07	0.01	-0.17	-0.24	-0.12
Evapotranspiration	761.23	783.19	786.77	795.56	799.78	801.38	2.88	0.46	1.12	0.53	0.20

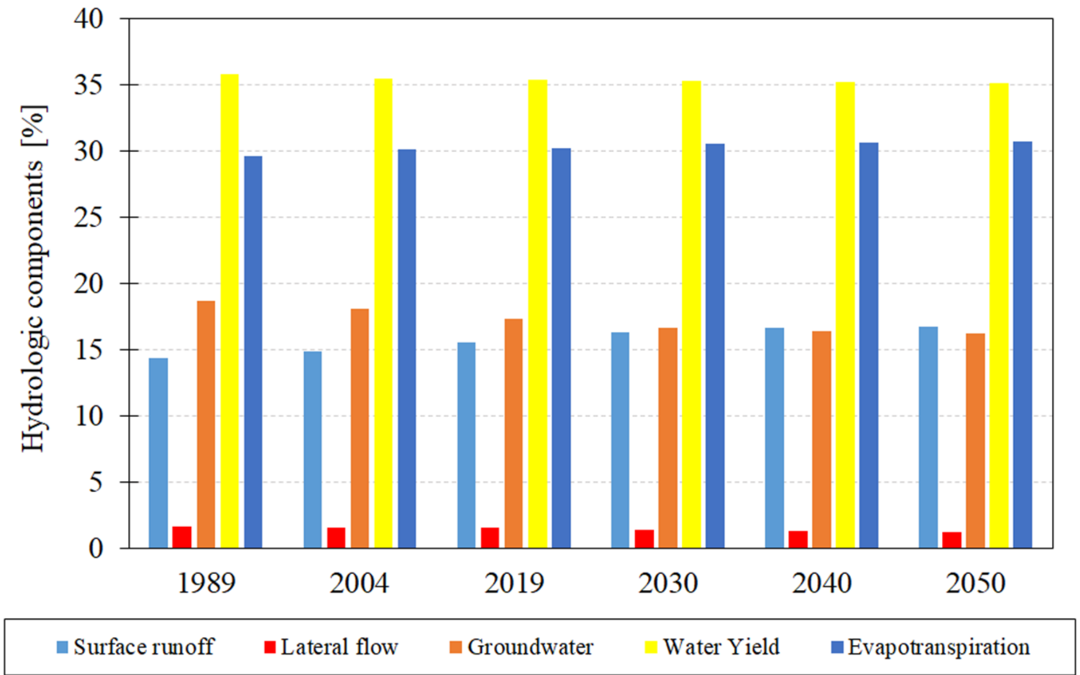

Figure 9. Annual hydrological components in the Fincha watershed.

3.4 Spatial Analysis of Watershed Hydrological Response to LULC Changes

Figure 10 shows the variations in hydrological responses from 1989 to 2004 (Fig. 10a) and 2004 to 2019 (Fig. 10b). Using LULC data from 1989 to 2019 for the previous 30 years, the amount and direction of the change in the hydrological response in each of the sub-watersheds were computed.

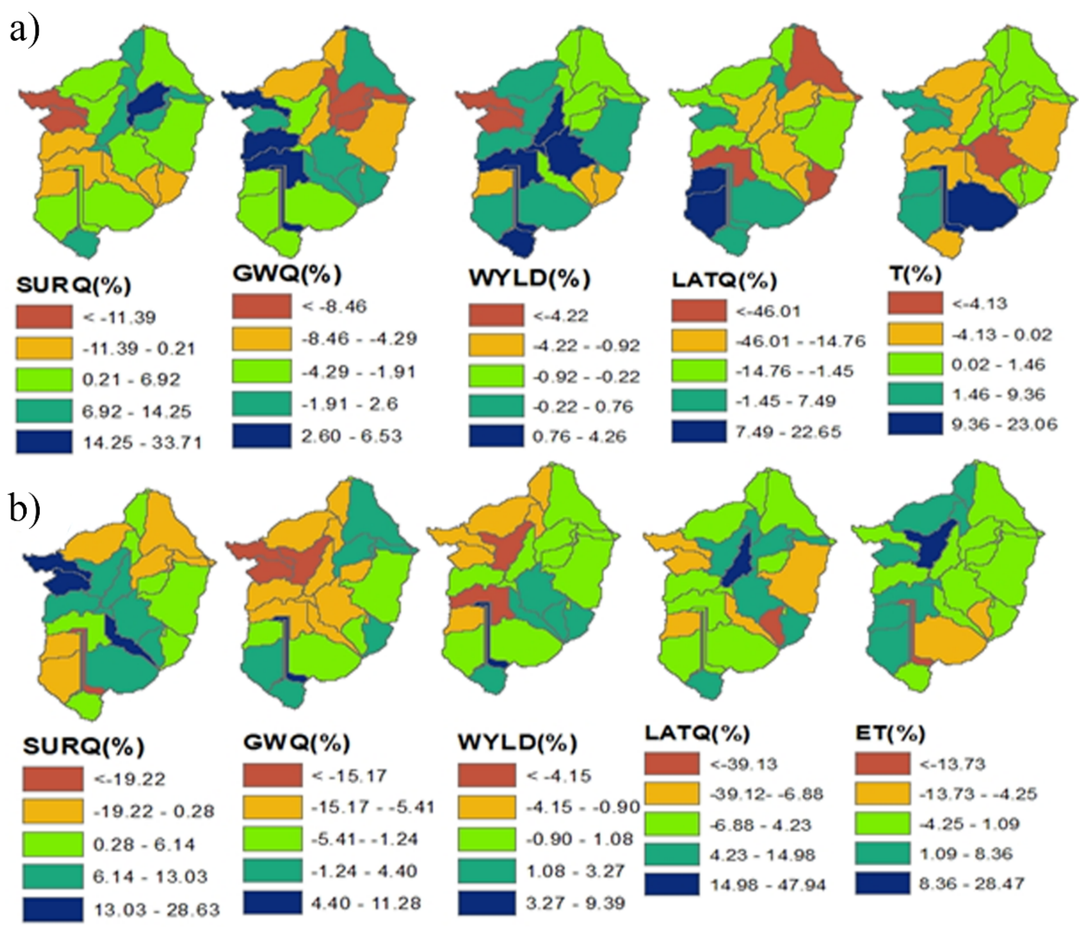

Figure 10. Spatial distribution of hydrological components changes at the sub-basin level for the periods a) 1989-2004 and b) 2004-2019. SURQ=Surface runoff; GWQ=Groundwater flow; WYLD=Water yield; LATQ=Lateral flow; ET=Evapotranspiration

Figure 11 indicates future changes in hydrological responses: 2019-2030 (Fig. 11a), 2030-2040 (Fig. 11b), and 2040-2050 (Fig. 11c), calculated using LULC data from the next thirty years.

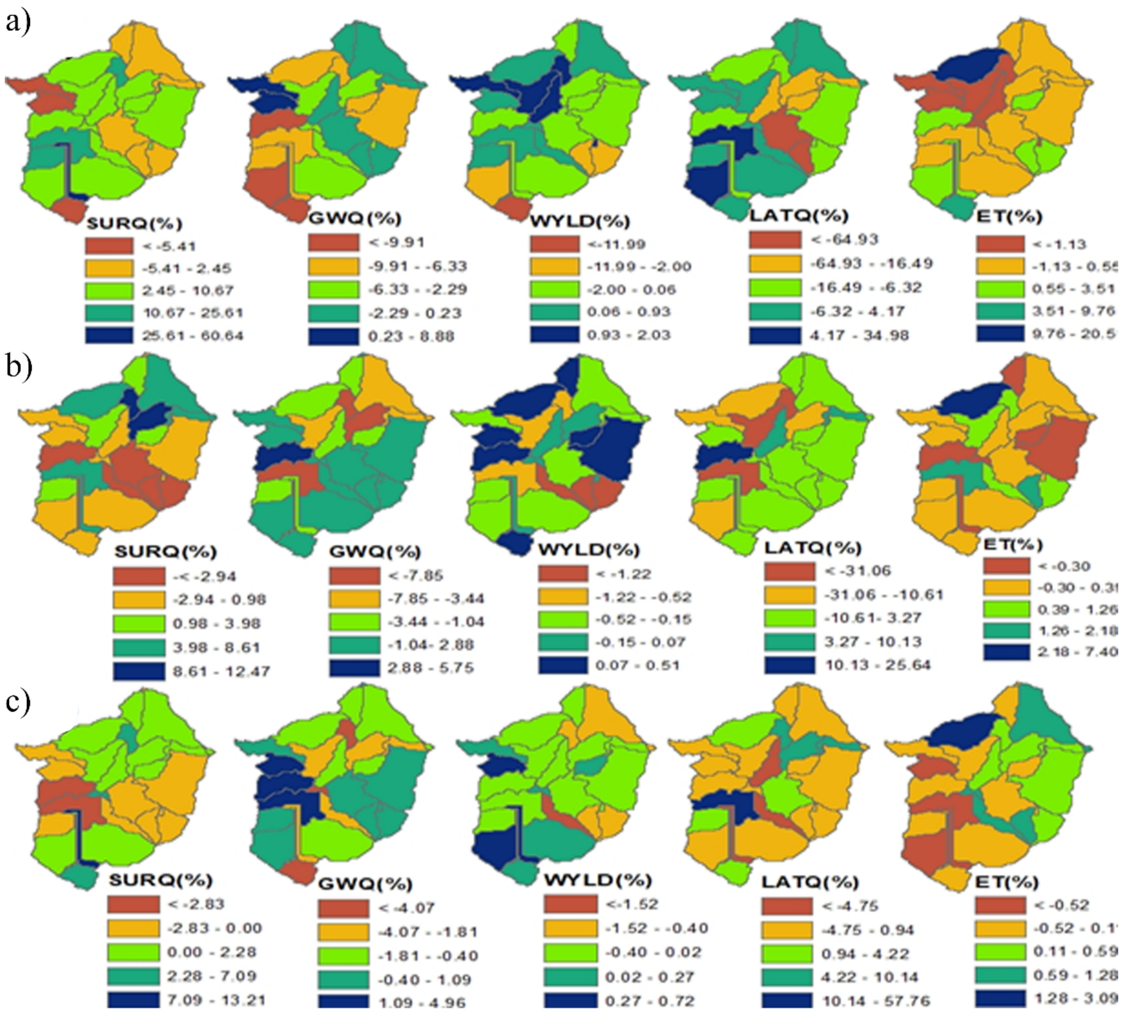

Figure 11. Spatial distribution of hydrological components changes at the sub-basin level for the periods a) 2019-2030, b) 2030-2040 and c) 2040-2050. SURQ=Surface runoff; GWQ=Groundwater flow; WYLD=Water yield; LATQ=Lateral flow; ET=Evapotranspiration

4. Discussion

The present study focused on evaluating the effect of past and future LULC conditions on the hydrological response of the Fincha watershed. This was done to provide additional science-based evidence to variations observed locally, mostly driven by a combination of natural factors and political decisions. Across the Fincha watershed, forest and shrub/sparse forests declined in the last three decades, and urban areas and agricultural land expanded rapidly as a consequence of significant internal relocation for economic reasons. At the same time, due to the construction of new water infrastructures (Amerti and Fincha dams) in the Fincha watershed, the water body class also increased. These new waterbodies contributed to further changing the landscape from the natural one (forests) to one dominated by agricultural fields and settlements.

Assuming that, in the future, the region will be developed similarly to what was observed in the past thirty years, the amount of agricultural land, urban areas, and forest cover will continue to grow (Regasa & Nones, 2022), which will result in increased yearly surface runoff and decreased lateral and groundwater flows. An increase is also expected in evapotranspiration, while water yield is expected to decrease, eventually affecting water resources at the watershed scale. In fact, deforestation, expansion of urban settlements, and agricultural development are positively correlated with surface runoff, while they are negatively correlated with groundwater and lateral flow. The present findings are consistent with Demissie (2022), who analyzed three hydrologic parameters (surface runoff, groundwater, and base flow), showing that all of them were negatively impacted by LULC changes, with surface runoff being the most affected.

It is worth noticing that each sub-watershed has its own unique hydrological process characteristics, and the spatiotemporal impact of LULC depends on them (Dibaba et al., 2020). The vulnerability degree of water resources is correlated to local LULC change (Kidane et al., 2019; Kenea et al., 2021), as one can recognize from the proportionality between the increase in surface runoff and urban and agricultural expansion.

In fact, under the first historical scenario (1989-2004), the western part of the study area shows a decrease in surface runoff, while the eastern and central parts exhibit the biggest increase (Figure 10a). However, in the second scenario (2004-2019) the eastern part increases in surface runoff while the southern part falls (Figure 10b). Areas with a high drop in surface runoff indicate a rise in groundwater, demonstrating that the link between surface runoff and groundwater is inverse under both conditions. For the first and second scenarios, a portion of the watershed's eastern and southern regions exhibit a high drop, which is in line with the work of Leta et al. (2020). In both the first and second scenarios, the water yield exhibits a sharp fall in the western and southwestern halves, respectively. However, in both cases, the water output is higher in the majority of the sub-basins. For the first and second scenarios, the lateral flow is particularly high in several southwest and central regions. Similar results are seen for the near future scenario (2019-2030), with some southwestern and northern regions showing the highest increases in surface runoff. The western and eastern portions of the country show the greatest drop in surface runoff in the second scenario (2030–2040), while the eastern portion shows the greatest increase (Figure 11b). Similarly, the surface runoff highly increased in some parts of the southern and shows a decrease in south-western parts in the third scenario. The groundwater is increased in western parts for all scenarios. But the area of increase is large in the third scenario (2040-2050) while the coverage of the increase of water yield is high in the second scenario (Figure 11c). The western and northern parts show a high increase in evapotranspiration in all scenarios, while areas located in =the eastern and southern parts of the region are likely to be affected by a decrease in evapotranspiration under the first and second scenarios.

In terms of the study's limitations, it is worth remembering that this investigation was performed in a data-scarce region. Thus, due to the lack of current data from the Ethiopian Ministry of Water and Energy (MOWE), the stream flow data for calibration and validation is limited to the year 2008. Therefore, this may not account for the recent development of hydraulic infrastructure like irrigation systems (Soressa & Gebre-Egziabher, 2023).

The sensitivity of the SWAT parameters was evaluated using the *p*-value and the *t*-stat value, and each parameter was then ranked, with rank 1 denoting the most sensitive parameter. In statistics, a parameter's significance is indicated by larger absolute *t*-statistics and lower *p*-values. At the same time, a high *p*-value suggests that there is no relationship between the response variable and changes in the predictor values (Tankpa et al., 2021). In the present study, V_GW_DELAY.gw (groundwater delay), R_CN2.mgt (SCS runoff curve number II), and V_GWQMN.gw (threshold depth of water in the shallow aquifer needed for reoccurrence flow to occur) are the top three most sensitive parameters, and control the stream routing and processes involving surface hydrology. According to the study conducted by Leta et al. (2021) in another Ethiopian watershed, the more sensitive parameters are CN2.mgt, GW_DELAY.gw, and SOL_K(1).sol. On the other hand, according to the result reported by Dibaba et al. (2020), CN2 (moisture condition II curve number), SOL_AWC (available water capacity of the soil layer) and RCHRG_DP (deep aquifer percolation fraction) are the three most top sensitive parameters.

5. Conclusions

The present study was carried out to simulate numerically how LULC changes will affect future hydrological conditions across the Fincha watershed in Ethiopia. The study offered crucial details about the relative effects of LULC on hydrological elements at the watershed and sub-watershed scales. Because of an increase in human-driven LULC conditions (agricultural fields, settlements) at the expense of natural landscapes like forests, surface runoff has historically increased at the watershed level, whereas groundwater and lateral flow have decreased. When examining each sub-watershed, regions with a sharp decline in surface runoff point to an increase in groundwater flow, demonstrating the inverse relationship between groundwater and surface runoff. The increase in surface runoff, and the consequent decrease of groundwater and lateral flow, could be due to the continued increase of agricultural land and urban areas and the extraction of forest cover from time to time indicated in a previous study (Regasa & Nones, 2022). The decline of both groundwater and lateral flow and the increase in surface runoff could pose a serious problem for agriculture, as more water is needed for irrigation during the dry season.

Without implementing proper management strategies and conservation policies, the trends highlighted here are like to continue in the future, negatively impacting the Ethiopian landscape and the local water resources.

This study provides more evidence on the impact of LULC changes on watershed hydrology, helping in developing effective water resource management strategies, that are needed to eventually tackle LULC-driven problems such as floods and droughts, soil erosion, and excessive sedimentation in water bodies. Future studies shall focus on the modelling of the combined impacts of LULC changes and climate changes on the Fincha watershed, aiming to not only compare the new results with the current results, but also to provide stakeholders with additional information on the future evolution of the region.

Author Contributions

Conceptualization M.S.R. and M.N.; writing-original draft preparation M.S.R. and M.N.; writing-revision M.S.R and M.N; literature review M.S.R. and M.N.; modelling M.S.R.; data analysis by M.S.R.; supervision M.N.; project management M.N.; funding acquisition M.N.

Funding

The NCN National Science Centre Poland-call PRELUDIUM BIS-1, Grant Number 2019/35/O/ST10/00167, provided funding for this study. Project website: https://sites.google.com/view/lulc-fincha/home.

Data availability

The data used in the present research are available on the IG PAS Data Portal (dataportal.igf.edu.pl) and from the corresponding author.

Conflicts of interests/Competing interests

On behalf of all authors, the corresponding author states that there is no conflict of interest.

References

Aawar, T., & Khare, D. (2020). Assessment of climate change impacts on streamflow through hydrological model using SWAT model: a case study of Afghanistan. Modeling Earth Systems and Environment, 6(3), 1427-1437. https://doi.org/10.1007/s40808-020-00759-0

Abdurahman, A., Yirsaw, E., Nigussie, W., & Hundera, K. (2023). Past and Future Land-use/Land-cover Change Trends and Its Potential Drivers in Koore's Agricultural Landscape, Southern Ethiopia. Geocarto International, 38(1), 2229952 https://doi.org/10.1080/10106049.2023.2229952

Abuhay, W., Gashaw, T., & Tsegaye, L. (2023). Assessing impacts of land use/land cover changes on the hydrology of Upper Gilgel Abbay watershed using the SWAT model. Journal of Agriculture and Food Research, 12, 100535. https://doi.org/10.1016/j.jafr.2023.100535

Agashua, L. O., Oluyemi-Ayibiowu, B. D., Ihimekpen, N. I., & Igibah, E. C. (2022). Modeling the semivariogram of climatic scenario around rivers by using stream network mapping and hydrological indicator. Journal of Human, Earth, and Future, 3(1), 17-31. https://doi.org/10.28991/HEF-2022-03-01-02

Al Khoury, I., Boithias, L., & Labat, D. (2023). A Review of the Application of the Soil and Water Assessment Tool (SWAT) in Karst Watersheds. Water, 15(5), 954. https://doi.org/10.3390/w15050954

Aragaw, H. M., Goel, M. K., & Mishra, S. K. (2021). Hydrological responses to human-induced land use/land cover changes in the Gidabo River basin, Ethiopia. Hydrological Sciences Journal, 66(4), 640-655. https://doi.org/10.1080/02626667.2021.1890328

Baker, T. J., & Miller, S. N. (2013). Using the Soil and Water Assessment Tool (SWAT) to assess land use impact on water resources in an East African watershed. Journal of Hydrology, 486, 100-111. https://doi.org/10.1016/j.jhydrol.2013.01.041

Barman, L., Prasad, R. K., & Sivakumar, B. (2023). Streamflow simulation using Soil and Water Assessment Tool (SWAT): application to Periyar River basin in India. ISH Journal of Hydraulic Engineering, 1-14. https://doi.org/10.1080/09715010.2023.2181673

Berihun, M. L., Tsunekawa, A., Haregeweyn, N., Meshesha, D. T., Adgo, E., Tsubo, M., ... & Yibeltal, M. (2019). Exploring land use/land cover changes, drivers and their implications in contrasting agro-ecological environments of Ethiopia. Land Use Policy, 87, 104052. https://doi.org/10.1016/j.landusepol.2019.104052

Cuceloglu, G., Abbaspour, K. C., & Ozturk, I. (2017). Assessing the water-resources potential of Istanbul by using a soil and water assessment tool (SWAT) hydrological model. Water, 9(10), 814. https://doi.org/10.3390/w9100814

Cuo, L., Lettenmaier, D. P., Mattheussen, B. V., Storck, P., & Wiley, M. (2008). Hydrologic prediction for urban watersheds with the Distributed Hydrology–Soil–Vegetation Model. Hydrological Processes, 22(21), 4205-4213. https://doi.org/10.1002/hyp.7023

Demissie, T. A. (2022). Land use and land cover change dynamics and its impact on watershed hydrological parameters: the case of Awetu watershed, Ethiopia. Journal of Sedimentary Environments, 7(1), 79-94. https://doi.org/10.1007/s43217-021-00084-1

Desalegn, T., Cruz, F., Kindu, M., Turrión, M. B., & Gonzalo, J. (2014). Land-use/land-cover (LULC) change and socioeconomic conditions of local community in the central highlands of Ethiopia. International Journal of Sustainable Development & World Ecology, 21(5), 406-413. https://doi.org/10.1080/13504509.2014.961181

Dibaba, W. T., Demissie, T. A., & Miegel, K. (2020). Drivers and implications of land use/land cover dynamics in Finchaa catchment, northwestern Ethiopia. Land, 9(4), 113. https://doi.org/10.3390/land9040113

Eshete, D. G., Rigler, G., Shinshaw, B. G., Belete, A. M., & Bayeh, B. A. (2022). Evaluation of streamflow response to climate change in the data-scarce region, Ethiopia. Sustainable Water Resources Management, 8(6), 187. https://doi.org/10.1007/s40899-022-00770-6

Etter, A., McAlpine, C., Wilson, K., Phinn, S., & Possingham, H. (2006). Regional patterns of agricultural land use and deforestation in Colombia. Agriculture, ecosystems & environment, 114(2-4), 369-386. https://doi.org/10.1016/j.agee.2005.11.013

Garg, V., Nikam, B. R., Thakur, P. K., Aggarwal, S. P., Gupta, P. K., & Srivastav, S. K. (2019). Human-induced land use land cover change and its impact on hydrology. HydroResearch, 1, 48-56. https://doi.org/10.1016/j.hydres.2019.06.001

Gurara, M. A., Jilo, N. B., & Tolche, A. D. (2023). Modelling climate change impact on the streamflow in the Upper Wabe Bridge watershed in Wabe Shebele River Basin, Ethiopia. International Journal of River Basin Management, 21(2), 181-193. https://doi.org/10.1080/15715124.2021.1935978

Gyamfi, C., Ndambuki, J. M., & Salim, R. W. (2016). Application of SWAT model to the Olifants Basin: calibration, validation and uncertainty analysis. Journal of Water Resource and Protection, 8(03), 397. https://doi.org/10.4236/jwarp.2016.83033

Katna, A., Thaker, M., & Vanak, A. T. (2023). How fast do landscapes change? A workflow to analyze temporal changes in human-dominated landscapes. Landscape Ecology, 1-11. https://doi.org/10.1007/s10980-023-01686-y

Kenea, U., Adeba, D., Regasa, M. S., & Nones, M. (2021). Hydrological responses to land use land cover changes in the fincha'a watershed, Ethiopia. Land, 10(9), 916. https://doi.org/10.3390/land10090916

Khalid, K., Ali, M. F., Abd Rahman, N. F., Mispan, M. R., Haron, S. H., Othman, Z., & Bachok, M. F. (2016). Sensitivity analysis in watershed model using SUFI-2 algorithm. Procedia Engineering, 162, 441-447. https://doi.org/10.1016/j.proeng.2016.11.086

Kidane, M., Tolessa, T., Bezie, A., Kessete, N., & Endrias, M. (2019). Evaluating the impacts of climate and land use/land cover (LU/LC) dynamics on the Hydrological Responses of the Upper Blue Nile in the Central Highlands of Ethiopia. Spatial Information Research, 27, 151-167. https://doi.org/10.1007/s41324-018-0222-y

Kouassi, J. L., Gyau, A., Diby, L., Bene, Y., & Kouamé, C. (2021). Assessing land use and land cover change and farmers' perceptions of deforestation and land degradation in South-West Côte d'Ivoire, West Africa. Land, 10(4), 429. https://doi.org/10.3390/land10040429

Kuma, H. G., Feyessa, F. F., & Demissie, T. A. (2023). Assessing the impacts of land use/land cover changes on hydrological processes in Southern Ethiopia: The SWAT model approach. Cogent Engineering, 10(1), 2199508. https://doi.org/10.1080/23311916.2023.2199508

Leta, M. K., Demissie, T. A., & Tränckner, J. (2021). Modeling and prediction of land use land cover change dynamics based on land change modeler (Lcm) in nashe watershed, Upper Blue Nile basin, Ethiopia. Sustainability, 13(7), 3740. https://doi.org/10.3390/su13073740

Leta, M. K., Demissie, T. A., & Tränckner, J. (2021). Hydrological responses of watershed to historical and future land use land cover change dynamics of Nashe watershed, Ethiopia. Water, 13(17), 2372. https://doi.org/10.3390/w13172372

Līcīte, I., Popluga, D., Rivža, P., Lazdiņš, A., & Meļņiks, R. (2022). Nutrient-rich organic soil management patterns in light of climate change policy. Civil Engineering Journal, 8(10), 2290-2304. https://doi.org/10.28991/CEJ-2022-08-10-017

Neitsch, S. L., Arnold, J. G., Kiniry, J. R., & Williams, J. R. (2011). Soil and water assessment tool theoretical documentation version 2009. Texas Water Resources Institute.

Maru, H., Haileslassie, A., Zeleke, T., & Teferi, E. (2023). Analysis of the impacts of land use land cover change on streamflow and surface water availability in Awash Basin, Ethiopia. Geomatics, Natural Hazards and Risk, 14(1), 1-25. https://doi.org/10.1080/19475705.2022.2163193

Megersa, T., Nedaw, D., & Argaw, M. (2019). Combined effect of land use/cover types and slope gradient in sediment and nutrient losses in Chancho and Sorga sub watersheds, East Wollega Zone, Oromia, Ethiopia. Environmental Systems Research, 8, 1-14. https://doi.org/10.1186/s40068-019-0151-3

Niyazi, B., Khan, A. A., Masoud, M., Elfeki, A., Basahi, J., & Zaidi, S. (2022). Optimum parametrization of the soil conservation service (SCS) method for simulating the hydrological response in arid basins. Geomatics, Natural Hazards and Risk, 13(1), 1482-1509. https://doi.org/10.1080/19475705.2022.2080005

Nyakundi, R., Nyadawa, M., & Mwangi, J. (2022). Effect of recharge and abstraction on groundwater levels. Civil Engineering Journal, 8(5), 910-925. https://doi.org/10.28991/CEJ-2022-08-05-05

Pennock, D. (2019). Soil erosion: The greatest challenge for sustainable soil management.

Regan, R. S., Markstrom, S. L., Hay, L. E., Viger, R. J., Norton, P. A., Driscoll, J. M., & LaFontaine, J. H. (2018). Description of the national hydrologic model for use with the precipitation-runoff modeling system (prms) (No. 6-B9). US Geological Survey. https://doi.org/10.3133/tm6B9

Regasa, M. S., Nones, M., & Adeba, D. (2021). A review on land use and land cover change in Ethiopian basins. Land, 10(6), 585. https://doi.org/10.3390/land10060585

Regasa, M. S., & Nones, M. (2022). Past and future land use/land cover changes in the Ethiopian Fincha Sub-Basin. Land, 11(8), 1239. https://doi.org/10.3390/land11081239

Regasa, M. S., & Nones, M. (2023). SWAT model-based quantification of the impact of land use land cover change on sediment yield in the Fincha watershed, Ethiopia. Frontiers in Environmental Sciences 11, 1146346. https://doi.org/10.3389/fenvs.2023.1146346

Rodríguez Eraso, N., Armenteras-Pascual, D., & Alumbreros, J. R. (2013). Land use and land cover change in the Colombian Andes: dynamics and future scenarios. Journal of Land Use Science, 8(2), 154-174. https://doi.org/10.1080/1747423X.2011.650228

Schielein, J., & Börner, J. (2018). Recent transformations of land-use and land-cover dynamics across different deforestation frontiers in the Brazilian Amazon. Land use policy, 76, 81-94. https://doi.org/10.1016/j.landusepol.2018.04.052

Soressa, T., & Gebre-Egziabher, T. (2023). Hydroelectric power dam-induced land use land cover change in Ethiopia, the case of AMerti-Nashe dams Horo Guduru Wollega Zone. African Geographical Review, 1-21. https://doi.org/10.1080/19376812.2022.2162093

Shitu, K., & Berhanu, S. (2023). Modeling the impact of changing in climatic variables on streamflow of Borkena River catchment, Awash Basin, Ethiopia. International Journal of River Basin Management, in press. https://doi.org/10.1080/15715124.2023.2200005

Tadesse, W., Whitaker, S., Crosson, W., & Wilson, C. (2015). Assessing the impact of land-use land-cover change on stream water and sediment yields at a watershed level using SWAT. Open Journal of Modern Hydrology, 5(03), 68. https://doi.org/10.4236/ojmh.2015.53007

Tankpa, V., Wang, L., Awotwi, A., Singh, L., Thapa, S., Atanga, R. A., & Guo, X. (2021). Modeling the effects of historical and future land use/land cover change dynamics on the hydrological response of Ashi watershed, northeastern China. Environment, Development and Sustainability, 23, 7883-7912. https://doi.org/10.1007/s10668-020-00952-2

Tola, S. Y., & Shetty, A. (2023). Quantification of change in land cover and rainfall variability impact on flood hydrology using a hydrological model in the Ethiopian river basin. Environmental Earth Sciences, 82(10), 254. https://doi.org/10.1007/s12665-023-10929-9

Shi, Y., Xu, G., Wang, Y., Engel, B. A., Peng, H., Zhang, W., ... & Dai, M. (2017). Modelling hydrology and water quality processes in the Pengxi River basin of the Three Gorges Reservoir using the soil and water assessment tool. Agricultural water management, 182, 24-38. https://doi.org/10.1016/j.agwat.2016.12.007

Zhang, J., Zhang, M., Song, Y., & Lai, Y. (2021). Hydrological simulation of the Jialing River Basin using the MIKE SHE model in changing climate. Journal of Water and Climate Change, 12(6), 2495-2514. https://doi.org/10.2166/wcc.2021.253

Figure 1. Location of the Fincha watershed, Oromia Regional State's Horro Guduru Walaga Zone, Upper Blue Nile Basin, Ethiopia.

Figure 2. Study workflow.

Figure 3. Soil types characterizing the Fincha watershed.

Figure 4. 2019 LULC map of the Fincha watershed.

Figure 5. Classification of the Fincha watershed based on terrain slope.

Figure 6. River drainage system (blue lines) and sub-watersheds (red contours).

Figure 7. Historical (1989-2019) and predicted (2030-2050) LULC changes in the Fincha watershed.

Figure 8. Comparison between computed and measured stream flow at the Fincha Dam outlet, during the calibration (1989-2002) and validation (2003-2008) periods.

Figure 9. Annual hydrological components in the Fincha watershed.

Figure 10. Spatial distribution of hydrological components changes at the sub-basin level for the periods a) 1989-2004 and b) 2004-2019. SURQ=Surface runoff; GWQ=Groundwater flow; WYLD=Water yield; LATQ=Lateral flow; ET=Evapotranspiration

Figure 11. Spatial distribution of hydrological components changes at the sub-basin level for the periods a) 2019-2030, b) 2030-2040 and c) 2040-2050. SURQ=Surface runoff; GWQ=Groundwater flow; WYLD=Water yield; LATQ=Lateral flow; ET=Evapotranspiration

Table 1. Data and sources.

Data	*Type*	Resolution/year	*Source*
Digital Elevation Model	Spatial Data	30m / 2019	Ministry of Water and Energy (MOWE), Ethiopia

Land use land cover	Spatial Data	30m / 2019, 2030, 2040, 2050	2019 derived from Landsat images 2030, 2040, and 2050 predicted by Land Change Modeler (Regasa and Nones, 2022)
Soil	Spatial Data		Ministry of Water and Energy (MOWE), Ethiopia
Weather data	Temporal data	1986-2019	Meteorological National Agency, Ethiopia
Stream flow	Temporal data	1986-2008	Ministry of Water and Energy (MOWE), Ethiopia

Table 2. Stream flow characteristics with range and fitted value, as determined by the SUFI-2-based sensitivity study. The absolute value of the *p*-value was used to determine their ranking.

Rank	Parameter Name	Description	Calibration	
			t-stat	*p*-value
1	V_GW_DELAY.gw	Groundwater delay (days)	-9.891	0.000
2	R_CN2.mgt	SCS runoff curve number II	2.391	0.018
3	V_GWQMN.gw	Threshold depth of water in the shallow aquifer required for return flow to occur (mm H2O)	-2.022	0.045
4	R_CH_N2.rte	Manning's "n" value for the main channel	0.717	0.474
5	R_SOL_AWC(1).sol	Available water capacity of the 1st soil layer (mm H2O mm soil−1)	0.699	0.486
6	R_SOL_K(1).sol	Saturated hydraulic conductivity at the 1st soil layer (mm h−1)	0.255	0.799
7	R_SLSUBBSN.hru	Average slope length (m)	0.153	0.878
8	R_RCHRG_DP.gw	Deep aquifer percolation fraction	-0.099	0.921
9	V_ALPHA_BF.gw	Base flow alpha factor(1 day−1)	0.060	0.952

Table 3. Monthly stream flow during the calibration (1989-2002) and validation (2003-2008) periods.

	Statistical test	R^2	*NSE*	*PBIAS*
Stream flow	Calibration	0.83	0.83	8.3
	Validation	0.84	0.76	12.2

Table 4: Fincha watershed's average annual hydrological components.

Hydrological components	Hydrological components [mm]						Hydrological components change [%]				
	1989	2004	2019	2030	2040	2050	2004-1989	2019-2004	2030-2019	2040-2030	2050-2040
Surface runoff	370.13	385.25	405.15	424.99	433.09	435.14	4.08	5.17	4.90	1.90	0.47
Lateral flow	42.52	40.26	40.04	36.14	33.38	32.73	-5.32	-0.55	-9.73	-7.64	-1.94
Groundwater	480.73	469.09	450.51	433.89	426.76	423.43	-2.42	-3.96	-3.69	-1.65	-0.78

Water yield	920.35	920.95	921.07	919.53	917.34	916.25	0.07	0.01	-0.17	-0.24	-0.12
Evapotranspiration	761.23	783.19	786.77	795.56	799.78	801.38	2.88	0.46	1.12	0.53	0.20